J Mol Model (2013) 19:3233–3243
DOI 10.1007/s00894-013-1853-5

ORIGINAL PAPER

Study on the role of SBA-15 in the oxidative dehydrogenation of n-butane over vanadia catalyst using density functional theory

Nguyen Ngoc Ha · Ngo Duc Huyen · Le Minh Cam

Received: 23 January 2013 / Accepted: 15 April 2013 / Published online: 7 May 2013

Abstract The first step in the mechanism of n-butane oxidative dehydrogenation (ODH) on a V_4O_{10} cluster and V_4O_{10} supported SBA-15 is examined using DFT method. The activation and adsorption energies, oxidation state of V atoms are calculated. Over V_4O_{10} the obtained results indicate that the activation of C-H bond of methylene group can occur at both the terminal and the bridging oxygen atoms with similar barrier (21.5–22.5 kcal mol^{-1}). The role of SBA-15 (with and without modification by Al) in n-butane adsorption step has been studied in detail. SBA-15 itself has mild effect on the reaction process, but the substitution of silicon atoms by aluminum atoms results in an active supporter for V_2O_5 in ODH reaction. In that, the ratio of Si/Al will decide the direction of initial interaction steps between n-butane and catalyst surface and it will result in the selectivity of the reaction products.

Keywords Activation of C-H bond · DFT · ODH · SBA-15

Introduction

The extensive availability and low price of light alkanes are the main reasons which have led to their use in the synthesis of the corresponding olefins, used as raw materials in several processes of considerable industrial importance. In particular, the interest in converting n-butane is due to the importance of butenes and butadiene in international markets. There are two possible ways for converting alkane: direct dehydrogenation and oxidative dehydrogenation. Direct dehydrogenation is reversible and suffers from several limitations: it is an endothermic process that requires high temperatures. At these temperatures, the catalyst deactivates because of coke formation, thus necessitating periodic regeneration of the catalyst which increases the operating cost [1]. In the last decade the exothermic oxidative dehydrogenation (ODH) reactions which can successfully overcome most of the obstacles mentioned above have attracted much interest as a potential alternative route for production of alkenes [2–6].

ODH reaction of n-butane is quite complex, the key aspect of the technology is the development of the catalysts capable of activating only the C - H bonds of the alkane molecule in a flow of oxygen. Despite the large number of studies found in the open literature [7–14] some important aspects, such as the nature of the active sites, the kinetics and the mechanism of the reaction, the hydrocarbon activation process and the factors that determine selectivity, are not sufficiently clear.

Vanadium oxide is a well-established catalyst for selective oxidative dehydrogenation process and the catalytic behavior of vanadium can be improved by depositing on an appropriate support [5–19]. Vanadium supported on SBA-15 was reported to be a suitable catalyst in the ODH of propane and butane. SBA-15 is a mesoporous silica material with uniform hexagonal channels, a narrow pore size distribution (5–30 nm), high surface areas (800–1000 m^2/g), and considerable hydrothermal stability due to a sufficient thickness of the framework walls (31–64 Å) [20]. To gain insight into the dispersity and the nature of V species formed on SBA-15 supported vanadium catalysts a detailed characterization of the vanadium incorporated SBA-15 catalysts by scanning electron microscopy (SEM)/transmission electron microscopy (TEM), diffuse reflectance ultraviolet–visible spectroscopy (DR UV–vis), ^{15}V

N. N. Ha (✉) · N. D. Huyen · L. M. Cam
Department of Chemistry and Laboratory of Kinetics and Catalysis, Hanoi National University of Education, Hanoi, Vietnam
e-mail: hann@hnue.edu.vn

N. D. Huyen
e-mail: huyendhsp@yahoo.com.vn

L. M. Cam
e-mail: leminhcamsp@yahoo.com

nuclear magnetic resonance spectroscopy (NMR), H_2-temperature-programmed reduction (TPR), ultraviolet rama spectroscopy (UV-Raman), X-ray diffraction (XRD), Fourier transform infrared spectroscopy (FTIR spectroscopy) has been performed [21–23].

It has been proposed the ODH reaction of alkane over vanadium based catalysts that occurs follows a Mars-van Krevelen red-ox mechanism [24], in which surface V sites are reduced by hydrocarbon and followed by re oxidation with adsorbed O_2 from the gas phase. The involvement of lattice oxygen species has been confirmed by techniques such as temporal-analysis of products (TAP) [25], isotopic labeling studies [26] and also quantum chemical calculations [27]. In our previous study [28], the electronic density of states was applied to study the electron transfer process of the adsorption step in the oxidative dehydrogenation of propane on V_2O_5 (001) with the orientation of CH_2 group onto V_2O_5(001). The calculations revealed that the reaction occurred between C_3H_8 and V_2O_5 follows the oxidation-reduction mechanism that means it was preceded via the Mars-van Krevelen redox mechanism. From the principle of maximum overlap in molecular orbital theory it was concluded that the CH_2 group is more active than the CH_3 group and the type of the adsorption is a typically chemical adsorption.

Generally, there are three types of lattice oxygen on vanadium oxide surfaces [26, 27]: i, singly coordinated terminal oxygen O(1), which is a vanadyl oxygen (V=O); ii, two-coordinated oxygen O(2); and iii, three-coordinated oxygen, O(3). To date, it remains controversial what kind of oxygen is responsible for hydrocarbon oxidation. In the past few years, the mechanism of ODH of propane over vanadium based catalysts have been studied extensively using density functional theory (DFT) [27–33]. A detailed mechanism for ODH of propane on the V_2O_5 (001) surface with a V_4O_{10} cluster have been carried out by Cheng and co-workers [34]. They found that the V=O(1) sites play an essential role for all reaction steps and the rate-determining step corresponds to the first hydrogen abstraction from the methylene group by the terminal oxygen O(1) with an activation barrier of 29.6 kcal mol^{-1}. The reaction pathways in ODH of propane on the V_2O_5 (001) surface have also been studied utilizing DFT by Ha Nguyen et al. [35]. For the first step of the catalytic cycle, the adsorption of propane, nine reaction pathways were examined and three different sites were investigated, namely are the vanadyl oxygen O(1), two-fold, O(2) and three-fold O(3). The obtained calculations indicated that the active center for propane activation was a V=O(1) group. The initial interaction of C_3H_8 with an active center involved simultaneous abstraction of the first hydrogen from the methylene group by the vanadyl oxygen O(1). This step with the highest activation barrier of 23.3 kcal mol^{-1} was found to be the rate-determining step. All calculations showed that among three types of oxygen atoms on the V_2O_5 (001) surface, the vanadyl oxygen V=O sites play the crucial role for all reaction steps.

Although a number of theoretical studies of the electronic structure and bonding properties of pure vanadium oxide surface have been carried out the study of the influence of support on the catalytic behavior of vanadium oxides in alkane ODH is very rare. Khaliullin et al. [36] carried out a comparative study of the reaction energetic for a VO_4 active site supported on cluster models of the SiO_2, TiO_2 and ZrO_2 surfaces. They found activation energies that were much higher than those found experimentally, and also found little dependence of activation energy on the support material, which is also contrary to experiment. The investigation of Redfern et al. [37] for ODH of propane on the (010) surface, in both vanadium oxide cluster and a periodic slab, indicated similar energetic for the vanadyl V=O site and bridging V-O-V site. Their calculation suggested that the (010) surface V_2O_5 is unfavorable for propane ODH and other factors, such as the influence of a support material, are responsible for the experimentally observed catalytic activity of vanadium.

From our knowledge, there are very few (if any) theoretical studies on the mechanism of n-butane ODH over bulk V_2O_5 catalyst and vanadium based catalysts as well. Because of the considerable uncertainties in the detail of the reaction mechanism in atomic scale for these systems, our works have focused on the electronic and geometric structure of vanadium based catalysts. In the previous work [38] the effects of MgO to V_2O_5 catalyst in the rate-determining step, the C-H bond activation step were investigated. The aim of the present work is to preliminary investigate the effects of support composition on the adsorption of n-butane on the surface, an early step in n-butane ODH mechanism. SBA-15 is considered as the support and the active site for n-butane adsorption is taken to be cubic V_4O_{10}. Density functional theory (DFT) is used to determine the energetic of n-butane adsorption. The results of this study may provide insight into the questions concerning the activity of vanadium based catalysts and especially how structure can be related to catalytic performance.

Computational and model methodology

Computational methods All spin polarized calculations have been performed by using the DFT method with non-local, gradient-corrected DFT. The Perdew, Burke, and Ernzerhof (PBE) gradient-corrected functional [39] are employed in the calculation of the exchange-correlation energy. This method is implemented in SIESTA code [40]. The exchange-correlation (XC) functional PBE chosen is

much better than LDA for calculating barrier heights [41], some other XCs (such as TPSS, TPSSh, B3LYP,…) are slightly better than PBE but their performance are worse [42]. The double zeta basis plus polarization orbital (DZP) for valence electrons while core electron are "frozen" in their atomic state by using norm-conserving pseudo potentials [43] in its fully nonlocal (Kleinman-Bylander) form Troullier-Martins with mesh cutoff (real energy) defined to be the equivalent plane wave cutoff for the grid was 1,360 eV. The Brillouin-zone sampling is restricted to the Γ-point. All equilibrium structures are performed using Quasi Newton algorithm and the forces acting on the dynamic atoms all are smaller than 0.05 eV $Å^{-1}$. Transition states have been found out by the nudged elastic band (NEB) method [44, 45] with the forces acting on the dynamic atoms all are smaller than 0.1 eV $Å^{-1}$.

A comparison of some of the optimized geometrical parameters with experimental data for n-C_4H_{10} is presented in Table 1 and Fig. 1. The results indicate that the optimized distances and angles in the model are in good agreement with the experimental values.

Cluster models For SBA-15: geometries of silica rings in SBA-15 mesoporous molecular sieve were investigated using the density functional theory (DFT) by Wang et al. [20]. Their work demostrated that bicyclic model clusters are the main structural units to consitute the framework of SBA-15. The geometries of these model clusters were fully optimized at the level of B3LYP with the 6-31G(d) basis set available in Gaussian 03. Their harmonic vibration frequencies were also evaluated at the same level. Therefore, in this work, this model is employed as the model cluster of SBA-15 molecular sieve. As shown in Fig. 2a, the bicyclic model cluster is composed of two monocyclic silica rings and it is called the model 5-6-s. 5- and 6- represent the numbers of silicon of two silica rings, "s" means that two hydroxyls of the model are not adjacent, namely separated by other groups. The boundary atoms of the model cluster are saturated by hydrogen atoms. The model consists of 9 Si atoms, 16 H atoms and 12 O atoms making 37 atoms in total.

The V_4O_{10} cluster model (Fig. 2b) is of Td symmetry (singlet state) and has been used in some theoretical studies as an oxidant in oxidative dehydrogenation of light hydrocarbons [34, 46]. It is also found as the most stable cluster [47]. This cluster contains the vanadyl V=O(1) site and the V-O(2)-V site, but does not contain the three-fold coordinated oxygen O(3) site. All vanadium atoms in V_4O_{10} have a formal oxidation state of +5, thus one can consider the V_4O_{10} cluster is suitable for modeling the chemistry of the V_2O_5-(001) surface. The reason for choosing V_4O_{10} cluster instead of monomeric units VO_4 is that: according to the observation reported in the literature [48] only for very low coverage degree on amorphous SiO_2 or ordered mesopore SBA-15, isolated species of the type VO_4 are prevalent. Using X-ray absorption spectroscopy and performed a detailed XAFS data analysis, Walter et al. [49] indicated that independent of the V loading, in the range 2.7–10.8 wt.% the isolated VO_4 units are not the major vanadium oxide species present on the dehydrated V_xO_y/SBA-15 samples, and thus an isolated VO_4 model did not properly describe the local structure between 2 Å and 4 Å around vanadium centers in dehydrated V_xO_y/SBA-15. Therefore, we believe that the results from the V_4O_{10} model are directly applicable to mechanisms for vanadium based catalysts.

Figure 2b and Table 2 show the structural parameters of the singlet of V_4O_{10}. The calculated bond distances are: V=O(1) = 1.54 Å and V-O(2) = 1.79 Å, they are in good agreement with experimental values obtained for the bulk V_2O_5 (1.59 and 1.78 Å for V=O and V-O respectively) [34]. Periodic DFT calculations on the V_2O_5 (001) surface by Sauer et al. [50] also lead to 1.59 Å for the bond distance of V=O and 1.80 Å for the V-O bond.

Finally, a complex model for V_4O_{10} located on SBA-15 has been proposed. The calculated bond distances for V_4O_{10} unit bound to the support SBA-15 are presented in Fig. 2c and Table 2. The formation of the combined system is an exothermic process, indicating that it is easy to create this system. New chemical bonds Si-O(V) have been formed with a bond distance of about 1.678 Å. The initial bond lengths of V=O(1) and V-O(2) are slightly changed: the V=O(1) bond elongates by 0.009 Å and V-O(2) bond distance increases from 1.795 to 1.874 Å.

Results and discussion

In our work, V_4O_{10} cluster, V_4O_{10} supported on parent SBA-15 and V_4O_{10} supported on modified SBA-15 were considered to study the adsorption of n-butane.

Table 1 Selected structural parameters of C_4H_{10}: distances (*r*) in Å and angles (*a*) in degrees

Selected structural parameters		(C^1, C^2 and C^3 are successive)	
	rC-H	rC^2-C^3	aC^1-C^2-C^3
Present work	1.108	1.513	112.3
Experiment (http://cccbdb.nist.gov/)	1.114	1.531	113.8

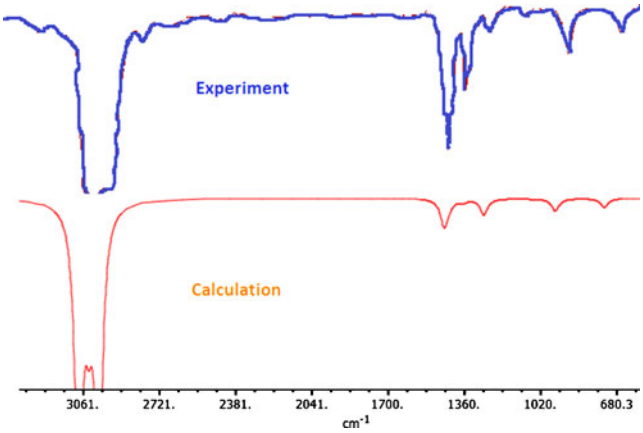

Fig. 1 IR spectrum of n-C_4H_{10}

According to Mars-van Krevelen, the first step is the initial activation of C_4H_{10} on the catalyst's surface. All calculations of activation energies and adsorption energies have been performed only for the initial step, the activation of C-H bond. Adsorption energy (E_{ads}) (or interaction energies) is calculated by equation:

$$Eads = E(C_4H_{10} + V_4O_{10}) - E(C_4H_{10}) - E(V_4O_{10}).$$

The adsorption of n-C_4H_{10} and C-H bond activation over V_4O_{10} and over V_4O_{10} supported on SBA-15 (V_4O_{10}/pureSBA-15)

The breaking of C-H bond can occur in the methyl ($-CH_3$) or the methylene ($-CH_2$) groups, therefore for the starting configuration, the butane molecule is located in front of V_4O_{10} or V_4O_{10}/pure SBA-15 with $-CH_2$ group (or $-CH_3$ group) is oriented directly toward to O-(V_4O_{10}) atom. Because V_4O_{10} cluster contains only two different lattice oxygens (named as O(1) and O(2)), starting from C_4H_{10} + V_4O_{10} (or C_4H_{10} + V_4O_{10}/pure SBA-15) four models of interactions between lattice oxygens and $-CH_2$ group or $-CH_3$ group are studied, i.e., O(1)…CH_2, O(1)…CH_3, O(2)…CH_2 and O(2)…CH_3. Furthermore for all investigated interaction models we assume an insertion mechanism [31, 35]: a lattice oxygen atom inserts into C-H bond of n-butane to form an alcoholic intermediate on the surface. The proton of the alcoholic intermediate is then transferred to another lattice oxygen.

The initial and final structures for each orientation are carefully optimized using Quasi Newton method then the CI-NEB is applied to find out the transition states. Calculated activation energies and adsorption energies for eight pathways (four paths for V_4O_{10} cluster and another four for V_4O_{10} supported on pure SBA-15) are shown in Table 3.

Reaction at O(1) site

- **O(1)....CH_2 interaction** involves the insertion of the vanadyl oxygen O(1) into a methylene C-H bond via a transition state ***Ts.V_4O_{10}*** over V_4O_{10} or via ***Ts.V_4O_{10}/SBA-15*** over V_4O_{10}/pureSBA-15.

– Over V_4O_{10}: the initial distances between C atom of $-CH_2$ group and O(1) is chosen by 3.036 Å; and the initial distances between H atom of C-H bond and O(1) is chosen by 2.157 Å. At ***Ts.V_4O_{10}*** (Fig. 3a) the C-H bond distance elongates from 1.108 to 2.089 Å and the H – O(1) distance is only 0.975 Å, indicating the OH group is nearly formed. The C…O(1) distance is decreased from 3.036 to 2.580 Å. The V=O(1) bond is lengthened from 1.542 to 1.785 Å. One of the three V–O(2) bonds distance decreases to 1.789 Å, while the other two bonds elongate to 1.810 and 1.813 Å. The activation barrier for this path is 21.5 kcal mol^{-1}, which is slightly higher than that over V_4O_{10}/pureSBA-15 and it is the second lowest barrier among eight studied pathways.

– Over V_4O_{10}/pureSBA-15: (Fig. 3b) At ***Ts.V_4O_{10}/SBA-15*** the C–H bond elongages from 1.108 to 1.796 Å and the distance between the H atom of CH_2 group and O(1) atom is shortened to 1.005 Å. The V=O(1) bond elongates from 1.551 to 1.756 Å. Two of three V – O(2) bonds distances decrease from 1.793 to 1.751 Å and from 1.874 to 1.806 Å, while the other increases from 1.791 to 1.819 Å. An E_{ads} value of –19.7 kcal mol^{-1} indicates this reaction is thermodynamically favorable. The activation barrier for this pathway is 19.3 kcal mol^{-1}, which is 2.2 kcal mol^{-1} lower than over V_4O_{10} and is the most energetically favorable path among eight studied reactions.

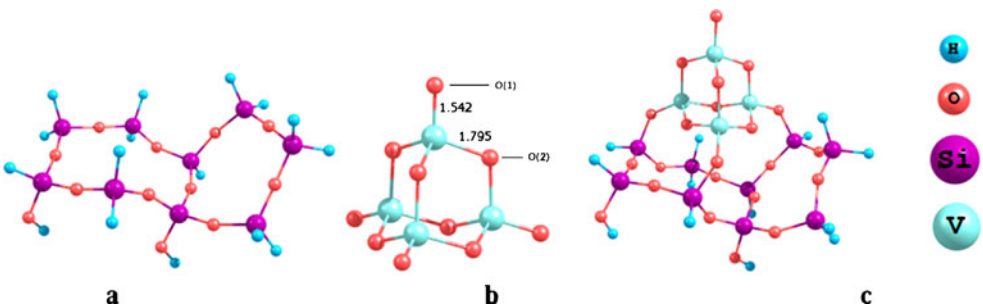

Fig. 2 Bicyclic model cluster of SBA-15 (**a**), V_4O_{10} (**b**) and combined system (**c**)

Table 2 Selected bond lengths for V_4O_{10} cluster, bicyclic model cluster of SBA-15 and V_4O_{10} supported on SBA-15

	V_4O_{10} cluster	Bicyclic model cluster of SBA-15	V_4O_{10}/SBA-15
Parameters (Å)			
d(V=O(1))	1.542	–	1.551
d(V-O(2))	1.795	–	1.874
d(Si-O_{butane})			1.677
d(Si-O_{SBA-15})		1.643	1.671

- **O(1)....CH_3 interaction** starts with inserting the O(1) into a methyl C-H bond. The calculations result in activation barriers of 33.6 kcal mol^{-1} and 35.4 kcal mol^{-1} for this reaction over V_4O_{10} and over V_4O_{10}/pureSBA-15 respectively, which are 12.1 kcal mol^{-1} and 16.1 kcal mol^{-1} higher than that of methylene C-H bond breaking. This observation is understandable because bonding energy of C-H in methylene group is 98.5 kcal mol^{-1}, which is weaker than that in methyl group (101.0 kcal mol^{-1}). Experimentally, isotopic studies by Chen et al. [9] indicated only the methylene C-H bond is involved in the rate determining step. Furthermore, iso-butyl radical is more stable than n-butyl radical due to the stronger hyperconjugation from CH_3 and CH_2 species. Overall this interaction is less favorable compared to the O(1)-CH_2.

Reaction at O(2) site

The pathways for this site are similar to those for the O(1) site. The calculation result for O(2)…CH_3 interaction over V_4O_{10} predicts an energy barrier of 5.4 kcal mol^{-1} higher than that for O(2)…CH_2 reaction indicating an energetically unfavored pathway on O(2) site. Therefore this path is not considered for the next discussion.

- **O(2)…CH_2 interaction:**

– Over V_4O_{10}: in this adsorption model the interaction involves the breaking of C-H bond and the formation of O-H bond via transition state ***Ts1.V_4O_{10}*** (Fig. 3c). Initially the n-butane molecule is placed in such a way that the distance between the O(2) and C atom is approximately 3.056 Å. After interaction, at transition state the C-H bond is weakened: the distance increases from 1.108 to 1.879 Å. The bond length of V-O(2) increases slightly from 1.795 to 1.819 Å. Especially, the ***Ts1.V_4O_{10}*** involves even O(1) site: the distance between H atom of C-H bond and O(1) is only 1.004 Å. In the intermediate's configuration, this distance decreases to 0.973 Å indicating the formation of OH group and also the C..O(2) distance is shortened to 1.480 Å. A low adsorption energy (−29.2 kcal mol^{-1}) could come from the requirement of two O sites in the adsorption state. Therefore, thermodynamically, the adsorption state related to the O(2) site is generally more stable than that related to the O(1) site. The barrier for this path is 22.5 kcal mol^{-1}.

– Over V_4O_{10}/pureSBA-15 (Fig. 3d): After interaction, at transition state the V=O(1) elongates to 1.774 Å; the C-H bond distance of CH_2 elongates from 1.108 to 2.477 Å. The CH_2-O(1) distance is 2.771 Å, which is 0.6255 Å longer than that in the initial state (3.396 Å). The H atom (of CH_2 group) and O(1) comes closer with a distance of 0.982 Å and an adsorbed hydroxyl is formed in the intermediate complex (not shown). Like ***Ts1.V_4O_{10}***, the ***Ts1.V_4O_{10}/pureSBA-***15 is more stable than ***Ts.V_4O_{10}*** and ***Ts.V_4O_{10}/pureSBA-***15 due to the involvement of O(1) in the structure of transition state. The activation barrier for this path is 28.3 kcal mol^{-1}.

The adsorption of n-C_4H_{10} over V_4O_{10}/modified SBA-15 (by Al^{3+})

Since silicon is balanced by four surrounding oxygen atoms, pure SBA-15 is charge neutral. By substituting a silicon atom by an aluminum atom, the charge balance of the network is upset creating strong Brønsted acid site Al-O-H. The sources of Brønsted acidity in SBA-15 are bridged -OH, which consists of a H atom, bonded to the O atom that connects the tetrahedrally coordinated cations. Alteration of Si/Al ratio lead to variations in the catalytic activity and stability of framework. In order to see the influence of SBA-

Table 3 Ea and Eads corresponded to the interaction between lattice O(1), O(2) and n-butane in the adsorption process over studied catalysts

	Ea (kcal mol^{-1})				Eads (kcal mol^{-1})			
	-CH_2		-CH_3		-CH_2		-CH_3	
	O(1)	O(2)	O(1)	O(2)	O(1)	O(2)	O(1)	O(2)
V_4O_{10}	21.5	22.5	33.6	27.9	−17.2	−29.2	−15.7	−22.6
V_4O_{10}/pure SBA-15	19.3	28.3	35.4	30.2	−19.6	−25.5	−9.5	−21.4
V_4O_{10}/SBA-15(Si_8Al)	15.0	25.4	32.0	30.0	−20.5	−26.0	−10.4	−13.0
V_4O_{10}/SBA-15(Si_7Al_2)	41.1	22.9	24.3	14.1	2.4	−31.2	−11.9	−36.6

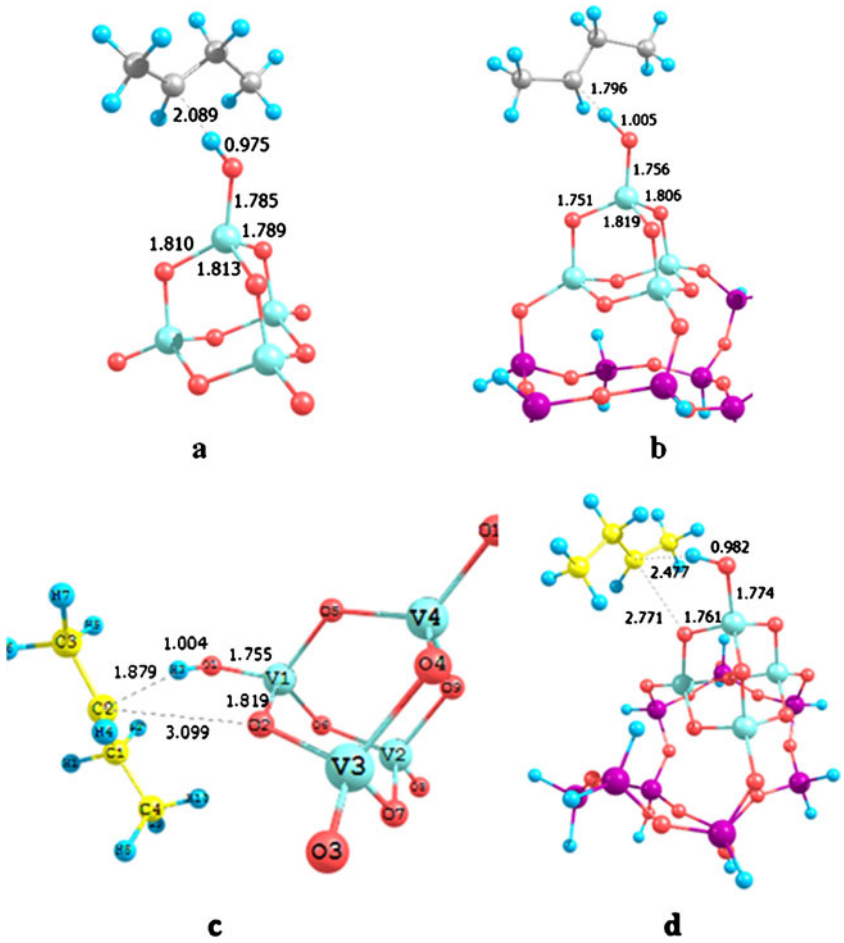

Fig. 3 Transition states of adsorption process with **a**: O(1)…CH_2 interaction over V_4O_{10}, **b**: O(1)...CH_2 interaction over V_4O_{10}/pure SBA-15; **c**: O(2)…CH_2 interaction over V_4O_{10}, **d**: O(2)…CH_2 interaction over V_4O_{10}/pure SBA-15

15 modification by aluminum on the adsorption process of n-butane, two different positions of silicon atom have been chosen for replacement by aluminum atoms. These positions are closest to the V atom to get the maximum influence of Al on the structure of V_4O_{10}. As one silicon atom has been substituted by aluminum, a Si/Al ratio of 8/1 was obtained and the modified SBA-15 is now named as SBA-15(Si_8Al); two silicon atoms have been substituted by aluminums, leading to SBA-15(Si_7Al_2) with a Si/Al ratio of 7/2.

We preliminary investigate the effect of aluminum atoms on the adsorption of n-butane over catalysts. For each model V_4O_{10}/SBA-15(Si_8Al) or V_4O_{10}/SBA-15(Si_7Al_2) four possible interactions between n-butane and V_4O_{10} are studied, including O(1)…CH_2; O(1)…CH_3; O(2)…CH_2 and O(2)…CH_3. These eight reaction pathways are similar to their O(n)…X counterparts above, and here we will mainly concentrate on their differences (n=1,2; X = $-CH_2$, $-CH_3$). The calculated energies for eight paths and selected optimized geometries are summarized in Table 3 and in Fig. 4. Like the situation over V_4O_{10} and V_4O_{10}/pure SBA-15, the calculated activation energies for recation pathways over two models indicate the preference of breaking methylene C-H bond over methyl C-H bond, thus the possibility of methyl C-H bond activation is not considered except the case of V_4O_{10}/SBA-15(Si_7Al_2) with O(2)…CH_3 interaction. Also the O(1)…CH_2 interaction over V_4O_{10}/SBA-15(Si_7Al_2) can be excluded because this path has the highest activation energy (41.1 kcal mol^{-1}) among all studied pathways.

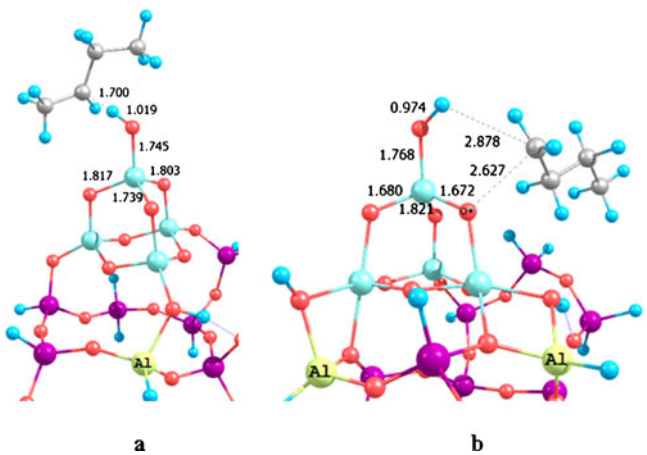

Fig. 4 Transition state of adsorption of n-C_4H_{10} over V_4O_{10}/SBA-15(Si_8Al) (**a**) and V_4O_{10}/SBA-15(Si_7Al_2) (**b**)

- **Over V_4O_{10}/SBA-15(Si_8Al)**: obviously, when SBA-15 is modified by one Al atom, the initial step for activation of methylene C-H bond seems to be easier than in the case of V_4O_{10} supported on pure SBA-15.

– O(1)…CH_2 reaction is the most energetically favored pathway with the lowest activation energy (15.0 kcal mol^{-1}) and the intermediate state in this reaction is stable due to a low negative adsorption energy (Eads = −20.5 kcal mol^{-1}). The related TS (named as ***Ts.V_4O_{10}/SBA-15(Si_8Al)***) is shown in Fig. 4a. At ***Ts.V_4O_{10}/SBA-15(Si_8Al)***, the C-H bond is lengthened to 1.700 Å and the O(1)-H distance is only 1.019 Å. The activation energy for this path is 6 kcal mol^{-1} and 4.3 kcal mol^{-1} lower than that in the O(1)…CH_2 reaction over V_4O_{10} cluster and V_4O_{10}/pureSBA-15, respectively. The V=O(1) bond length elongates to 1.745 Å. This TS is stabilized by hyperconjungtion from two CH_3 groups.

– The pathway of the O(2)…CH_2 is similar to their O(1)…CH_2 counterpart. This path has higher activation energy (25. 4 kcal mol^{-1}) than that in O(1)…CH_2 interaction, but its adsorption energy is 5.5 kcal mol^{-1} lower than that in O(1)…CH_2. The transition state of this reaction (not shown) consists of two O sites: O(2) and O(1) sites. Furthermore a low adsorption energy indicates the stability of the intermediate state. Therefore, compared to the pathway on the O(1) site the adsorption on the O(2) site is favorable in thermodynamics, but it is less favorable in kinetics.

- **Over V_4O_{10}/SBA-15(Si_7Al_2):** by contrast, when two aluminum atoms present (V_4O_{10}/SBA-15(Si_7Al_2)), the favorable adsorption sites for n-butane are near the O(2) sites and the energetically most favored path is the CH_3···O(2) with Ea being 14.1 kcal mol^{-1}. This path also has the lowest adsorption energy −36 kcal mol^{-1}. At TS the C-H bond distance is increased to 2.878 Å, the distance between C atom and O(2) is 2.627 Å, the distance between H atom of CH_3 group and O(1) is only 0.974 Å indicating an adsorbed hydroxyl is formed. A mild structural change is observed where two of three V-O(2) bond lengths are slightly shortened, while the other elongates to 1.821 Å. The V=O(1) bond length is 1.768 Å. Although the distance between $V_4O_{10}H$ and *n*-C_4H_9 is quite large (2.627 Å, Fig. 4b), but the $V_4O_{10}H$ is very stable due to significant shorteness of V-O bonds distances. Especially V-O^*(2) bond distance is decreased to 1.672 Å (it is 0.123 Å shorter than that in the case of V_4O_{10}cluster). This bond plays a major role in stabilizing thesystem because this site is in direct interaction with *n*-C_4H_9. In addition, while at ***Ts.V_4O_{10}/SBA-15(Si_8Al)*** *iso*-C_4H_9 directly links with SBA-15(Si_8Al)/$V_4O_{10}H$ only through H-O(1)=V bridge, at ***Ts.V_4O_{10}/SBA-15(Si_7Al_2)***, the methyl group of *n*-C_4H_9 has two simultaneous interactions: with the O(2) site and O(1) site, it may result in a closer to silica framework of *n*-C_4H_9 and consequently the transition state is stabilized with a low activation energy. Therefore one may suggest that when SBA-15 is modified by aluminum atoms the interaction between CH_3 group and O(2) site is the most favorable pathway of but−1-ene product formation.

Spectrum analysis of X-ray absorption near edge structure (XANES) on V atom in catalysts

Because ODH reaction is a redox process, C_4H_{10} is reduced by V^{+5} in catalyst. Theoretically, V atom with a higher oxidation number will be a more powerful oxidizer. Therefore, the detailed study of oxidation state of V atom in catalysts can give more information about the role of the modification of SBA-15 by Al.

Formal oxidation number of V in V_4O_{10}, V_4O_{10}/pureSBA-15, V_4O_{10}/SBA-15(Si_8Al_1) and V_4O_{10}/SBA-15(Si_7Al_2) is +5 but they are unmeasurable and their physical meaning can be ambiguous. The informal oxidation state (or spectroscopic oxidation state) can be measurable, this oxidation state of each atom changes depending on the chemical environment surrounding the atom. The XANES spectra can give useful information.

To compare the informal oxidation state of V, XANES K-edge of V atoms in studied catalysts have been calculated. K-edge spectrum of V consists of two parts: pre-edge: electron excited from 1s → 3d (the excitation of electron from 1s → 3d) and edge: 1s → 4p (the excitations $1s^{1/2}$ → $4p^{1/2}$ and $4p^{3/2}$, the experimental value of starting excitation energy of $K\beta_2$ edge of V in V_2O_5 crystal is about 5,475 eV [51, 52] according to the selection rules ($\Delta l=\pm1$). The obtained results are shown in Fig. 5, with V(1) and V(2) denoted for V atoms bound to O(1) and O(2) sites respectively.

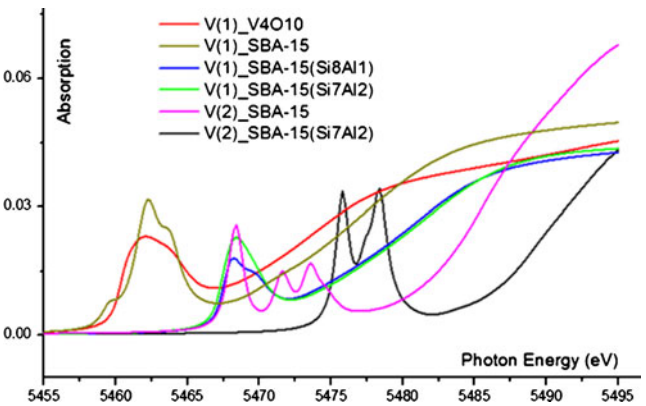

Fig. 5 K-edge spectra of V in catalysts

According to a fundamental property of the XANES spectrum, *the higher excitation energy is, the higher oxidation number should be*, the following comments may be useful:

(i) Informal oxidation states of V in V_4O_{10} cluster and V_4O_{10}/pure SBA-15 (without modification) are very similar due to the similarity in the values of starting excitation energies of K-edge (about 5,467 eV). It results in a similar activation barrier for the O(1)…CH_2 interaction over both V_4O_{10} and V_4O_{10}/pureSBA-15 (21.5 and 19.3 kcal mol^{-1}, Table 3).

(ii) When Silicon atoms in SBA-15 framework are substituted by aluminum atoms, informal oxidation state of V is significantly increased but these changes are different in V(1) and V(2).

- At V(1), K-edges are almost unchanged (about 5,472 eV) when the Si/Al ratio changes from 8/1 to 7/2.
- At V(2), K-edge is dramatically increased. For example, with a Si/Al ratio of 7/2, K-edge is increased up to 5,482 eV. This change in K-edge may result from the closer position of V(2) to aluminum atom compared to V(1). Therefore, the informal oxidation number of V(2) is higher than that of V(1). Over V_4O_{10}/SBA-15(Si_7Al_2), V(2) oxidizes C_4H_{10} more strongly than V(1) and obviously, the CH_3···O(2)-interaction is the most favored pathway with a very low activation energy (14.1 kcal mol^{-1}, Table 4).

The comparison with previous works and general comments on the initial step of n-butane ODH process over four studied catalytic systems

In previous work [35] the density functional theory using a plane-waves basis set and pseudo potential has been used to study the reaction pathways for ODH of propane on the V_2O_5 (001) surface. Our results revealed that the lowest energy pathway for propane activation occurred by an O(1) insertion into a methylene C-H bond of propane producing an iso-propanol structure. This agrees well with the conclusions from Gilardoni et al. [27] and Redfern et al. [37]. This step is the rate-determining step with activation energy of 23.3 kcal mol^{-1}. The subsequent step involved the abstraction of the second hydrogen by O(1) site leading to the formation of propene. This process had activation energy of 22.5 kcal mol^{-1}. The elimination of surface bound water molecule at the O(1) was a barrierless process. In that study, the electronic density of state has been applied to prove the reality of the calculated results.

In the following work [38], the effect of support MgO on the activity of V_2O_5 for ODH of propane and n-butane was investigated. In that work, only interaction of methylene group with the V_4O_{10}/MgO surface was considered. The activation energy for this step was found to be 30.8 kcal mol^{-1} and 32.9 kcal mol^{-1} for propane and n-butane respectively. The adsorption energies were −5.2 kcal mol^{-1} for both. According to obtained results one can see the initial step, the activation of C-H bond, becomes more difficult with V_4O_{10} supported MgO catalyst in both kinetics and the thermodynamics sides because of higher activation and adsorption energies in comparison to those in pure V_4O_{10}. The electron density, spin density, XANES were used to successfully explain the reasons for the difference in catalytic activity when V_2O_5 was located on the MgO.

On the basis of the barriers for initial activation in n-butane over vanadium oxide and vanadium oxide supported SBA-15 catalysts, the possible comments can be given as follows:

(i) It is expected that the initial step in n-butane ODH would be the interaction between methylene group and V=O(1) site or O(2) site. The negative values of adsorption energies obtained indicate initial step is thermodynamically favorable. Our results are similar with Fu et al. [31]. Their results demonstrated that both O(1) and O(2) species of vanadium oxide are active for C-H bond breaking but the O(1) was slightly more active than the O(2). From the calculated results it is hard to find a strong preference of the O(1) site over O(2) site in activation step of the C-H bond. Over V_4O_{10} the reaction barrier in the pathway of the O(1) site is only 1 kcal mol^{-1} lower than that of the O(2) site. But at site O(2) a 10 kcal mol^{-1} adsorption energy lower than that on O(1) site indicates the intermediate state in the O(2)…CH_2 reaction is more stable compared to its counterpart in the O(1)…CH_2 path. Therefore, compared to the pathway on the O(1) site, the dissociative adsorption on the O(2) site is more favorable in thermodynamics, and it could be competitive in kinetics.

(ii) A further analysis based on atomic charge is performed in order to understand more about the reducibility of the lattice O. Table 4 presents the atomic charge of selected

Table 4 The atomic charge of O surface atoms at clean surface and at the transition states related to O(1)…CH_2 interaction

TSs	O(1)		O(2)
	Clean surface	TS	Clean surface
Ts.V_4O_{10}	−0.163	−0.188	−0.198
Ts.V_4O_{10}/SBA-15	−0.187	−0.186	−0.214
Ts.V_4O_{10}/SBA-15(Si_8Al)	−0.177	−0.183	−0.200
Ts.V_4O_{10}/SBA-15(Si_7Al_2)	−0.195	−0.196	−0.235

surface atoms at clean surface and at transition states computed using Hirshfeld calculation, almost independent of basis set. The atomic charge reflects the ability of the lattice O to further gain electrons (reducibility). It is found that on the clean surface of all catalysts the atomic charges for O(2) atoms are more negative than that for O(1) atoms and are more difficult to be reduced, the O(1) atoms is more active. However, these atomic charges do not reflect the actual activity of the O(2) found out by our work. Our explaination is similar to Fu et al. [31]: If one looks at the intermediate state they will find that for all studied catalysts, calculated adsorption energies (Eads) related to O(2) site are always more negative than that related to O(1) site. That means, thermodynamically, the adsorption states related to O(2) sites are generally more stable. The analysis of transition states reveals that while in the transition states related to O(1) - C_4H_9 species link with the catalyst's surfaces through O(1) site only, the transition states related to O(2) site involve two O sites: the reacting lattice O(1) and O(2) and therefore it could be a factor to stabilize the transition state. Furthermore, although the O(2) has less ability to be reduced compared to O(1) it has a better contact with other surface atoms (two neighbour V atoms), while O(1) atom bonds only directly with one V atom. So the electron at the O(2) site can be well delocalized into the nearby atoms, this can help to stabilize the transition states.

(iii) The presence of silicalite SBA-15 as a support has a mild effect on the adsorption activity of V_4O_{10}: the calculated results reveal that SBA-15 has a positive effect only for the activation of methylene C-H bond at site O(1). For all other models, the activation of C-H bond becomes kinetically and thermodynamically more difficult due to slightly higher activation energies and adsorption energies observed.

However, with modification by Al atom, SBA-15 becomes an effective support for vanadium oxide in ODH process of n-butane. Table 4 shows that the atomic charge of O(1) atoms at transition states related to O(1)..CH_2 interaction shows a sequence of −0.183, −0.186, −0.188, −0.196 going from ***Ts.V_4O_{10}/SBA-15(Si_8Al); Ts.V_4O_{10}/SBA-15; Ts.V_4O_{10}*** and to ***Ts.V_4O_{10}/SBA-15(Si_7Al_2).*** Therefore the O(1) atom in ***Ts.V_4O_{10}/SBA-15(Si_7Al_2)*** is the most difficult to be reduced reflecting the highest activation energy (41.1 kcal mol^{-1}). By contrast, the O(1) atom at ***Ts.V_4O_{10}/SBA-15(Si_8Al)*** is the most active with the strongest electrophilic tendency (Ea=15 kcal mol^{-1}). It is also found that electrons are transfered from –CH_2 group to the surface V atom via bridge oxygen [28] and the electron transfer through ***Ts.V_4O_{10}/SBA-15*** is more favorable than through ***Ts.V_4O_{10}***.

Over V_4O_{10}/SBA-15(Si_7Al_2) the reaction between CH_3 group and O(2) site is the most favorable path in both thermodynamic and kinetic aspects for the C-H bond activation.

Conclusions

The reaction pathways for the first step in the mechanism of n-butane ODH process over vanadium oxide and vanadium oxide supported on SBA-15 have been studied utilizing DFT theory. Obviously, the cubic V_4O_{10} cluster is a good model for studying the catalysis on V_2O_5, particularly for supported catalysts. For the first step of the catalytic cycle, the adsorption of n-butane and the C-H bond activation, eight reaction pathways are examined and two different sites are investigated, namely the vanadyl oxygen O(1) and two-fold O(2). The obtained calculations indicate that the lowest energy pathway for n-butane activation occurred by an O(1) insertion into a methylene C-H bond of n-butane producing an iso-butanol structure with a barrier of 21.5 kcal mol^{-1}. The activation of a C-H bond in methyl goup is less possible. Furthermore, the calculated results reveal that the activation of C-H bond can also occur at the bridging oxygen atoms O(2). Compared to the pathway on the O(1) site, the dissociative adsorption on the O(2) site is more favorable in thermodynamics, and it could be competitive in kinetics.

The effect of SBA-15 on the catalytic activity of vanadium oxide is clarified: when V_4O_{10} setting up on pure SBA-15 the interaction of vanadium oxide with SBA-15 slightly lowers activation energy and adsorption energy for O(1)… CH_2 reaction. The substitution of SBA-15 by aluminum atoms create a more effective support for vanadium oxide in ODH process. The presence of aluminum atoms help stabilize the transition state and hence reduce the activation energies. When one Si is substituted by Al, the interaction between methylene group and terminal oxygen O(1) is more pronound and it is the lowest energy pathway, in which the C-H bond breaks to form an alcoholic intermediate with a barrier of 19.3 kcal mol^{-1}. However, when SBA-15 is modified by aluminum atoms the interaction between CH_3 group and O(2) site is the most favorable pathway. This path can lead to the formation of but-1-ene as the main product. In this direction, the activation barrier and also adsorption energy are quite low (Ea=14.1 kcal mol^{-1} and Eads= −36.6 kcal mol^{-1}).

Overall, the calculated results indicate that both O(1) and O(2) species of the catalyst are active for C-H bond breaking, but the O(1) site is slightly more active than O(2) site. However, the adsorption on site O(2) is more favorable in thermodynamics. The results of this study may provide the information for future computational investigations of these materials.

Acknowledgments This work was supported by National Foundation for Science and Technology Development Viet Nam (NAFOSTED) under project number 104.03-2010.39

References

1. Grabowski R (2006) Kinetics of oxidative dehydrogenation of C_2-C_3 alkanes on oxide catalysts. Catal Rev 48:199–268. doi:10.1080/01614940600631413
2. Wu Z, Kim HS, Stair PC, Rugmini S, Jackson SD (2005) On the structure of vanadium oxide supported on aluminas: UV and visible Raman spectroscopy, UV-visible diffuse reflectance spectroscopy, and temperature-programmed reduction studies. J Phys Chem B 109:2793–2800. doi:10.1021/jp046011m
3. Murgia V, Torres EM, Gottifredi JC, Sham EL (2006) Sol–gel synthesis of V_2O_5–SiO_2 catalyst in the oxidative dehydrogenation of n-butane. Appl Catal A 312:134–143. doi:10.1016/j.apcata.2006.06.042
4. Evans OR, Bell AT, Tilley TD (2004) Oxidative dehydrogenation of propane over vanadia-based catalysts supported on high-surface-area mesoporous $MgAl_2O_4$. J Catal 226:292–300. doi:10.1016/j.jcat.2004.06.002
5. Liu W, Lai SY, Dai H, Wang S, Sun H, Au CT (2007) Oxidative dehydrogenation of n -butane over mesoporous VO_x/SBA-15 catalysts. Catal Lett 113:147–154. doi:10.1007/s10562-007-9023-y
6. Madeira LM, Portela MF (2002) Catalytic oxidative dehydrogenation of n-butane. Catal Rev 44:247–286. doi:10.1081/CR-120001461
7. Dias PS, Dimitrov LD, Oliveira MCR, Zavoianu R, Fenandes A, Portela MF (2010) Oxidative dehydrogenation of butane over substoichiometric magnesium vanadate catalysts prepared by citrate route. J Non-Cryst Solids 356(28–30):1488–1497. doi:10.1016/j.jnoncrysol.2010.04.042
8. Sugiyama S, Hiratab Y, Nakagawa K, Sotowa KI, Maeharad K, Himenod Y, Ninomiya W (2008) Application of the unique redox properties of magnesium ortho-vanadate incorporated with palladium in the unsteady-state operation of the oxidative dehydrogenation of propane. J Catal 260:157–163. doi:10.1016/j.jcat.2008.09.015
9. Chen KD, Bell AT, Iglesia E (2002) The relationship between the electronic and redox properties of dispersed metal oxides and their turnover rates in oxidative dehydrogenation reactions. J Catal 209:35–42. doi:10.1006/jcat.2002.3620
10. Grabowski R, Słoczyński J (2005) Kinetics of oxidative dehydrogenation of propane and ethane on VOx/SiO_2 pure and with potassium additive. Chem Eng Process 44:1082–1093. doi:10.1016/j.cep.2005.03.002
11. Iannazzo V, Neri G, Galvagno S, Serio MD, Tesser R, Santacesaria E (2003) Oxidative dehydrogenation of isobutane over V_2O_5-based catalysts prepared by grafting vanadyl alkoxides on TiO_2-SiO_2 supports. Appl Catal A 246:49–68. doi:10.1016/S0926-860X(02)00668-3
12. Jackson SD, Rugmini S (2007) Dehydrogenation of n-butane over vanadia catalysts supported on θ-alumina. J Catal 251:59–68. doi:10.1016/j.jcat.2007.07.015
13. Solsona B, Ivars F, Concepción P, López Nieto JM (2007) Selective oxidation of n-butane over MoV-containing oxidic bronze catalysts. J Catal 250:128–138. doi:10.1016/j.jcat.2007.05.023
14. Marcu IC, Sandulescu I, Schuurman Y, Millet JMM (2008) Mechanism of n-butane oxidative dehydrogenation over tetravalent pyrophosphates catalysts. Appl Catal A 334:207–216. doi:10.1016/j.apcata.2007.09.049
15. Klisińska A, Samson K, Gressel I, Grzybowska B (2006) Effect of additives on properties of V_2O_5/SiO_2 and V_2O_5/MgO catalysts: I. Oxidative dehydrogenation of propane and ethane. Appl Catal A 309:10–16. doi:10.1016/j.apcata.2006.04.028
16. Fu YH, Ma HC, Wang Z, Zhu W, Wu T, Wang GJ (2004) Characterization and reactivity of SnO_2-doped V_2O_5/γ-Al_2O_3 catalysts in dehydrogenation of isobutane to isobutene. J Mol Catal A Chem 221:163–168. doi:10.1016/j.molcata.2004.07.016
17. Khodakov A, Olthof B, Alexis AT, Iglesia E (1999) Structure and catalytic properties of supported vanadium oxides: support effects on oxidative dehydrogenation reactions. J Catal 181:205–216. doi:10.1006/jcat.1998.2295
18. Went GT, Oyama ST, Bell AT (1990) Laser Raman spectroscopy of supported vanadium oxide catalysts. J Phys Chem 94:4240–4246. doi:10.1021/j100373a067
19. Kung HH (1994) Oxidative dehydrogenation of light (C_2 to C_4) alkanes. Adv Catal 40:1–38. doi:10.1016/S0360-0564(08)60655-0
20. Wang Z, Wang D, Zhao Z, Chen Y, Lan J (2011) A DFT study of the structural units in SBA-15 mesoporous molecular sieve. Comput Theor Chem 963:403–411. doi:10.1016/j.comptc.2010.11.004
21. Gruene P, Wolfram T, Pelzer K, Schlogl R, Trunschke A (2010) Role of dispersion of vanadia on SBA-15 in the oxidative dehydrogenation of propane. Catal Today 157:137–142. doi:10.1016/j.cattod.2010.03.014
22. Setnička M, Bulánek R, Čapek L, Čičmanec P (2011) n-Butane oxidative dehydrogenation over VO_x - HMS catalyst. J Mol Catal A 344:1–10. doi:10.1016/j.molcata.2011.05.004
23. Bulánek R, Kaluzova A, Setnicka M, Zukal A, Cicmanec P (2012) Study of vanadium based mesoporous silicas for oxidative dehydrogenation of propane and n-butane. Catal Today 179:149–158. doi:10.1016/j.cattod.2011.08.044
24. Cortés I, Rubio O, Herguido J, Menéndez M (2004) Kinetics under dynamic conditions of the oxidative dehydrogenation of butane with doped V/MgO. Catal Today 91–92:281–284. doi:10.1016/j.cattod.2004.03.044
25. Pantazidis A, Bucholz SA, Zanthoff HW, Schuurman Y, Mirodatos C (1998) A TAP reactor investigation of the oxidative dehydrogenation of propane over a V–Mg–O catalyst. Catal Today 40:207–214. doi:10.1016/S0167-2991(99)80141-4
26. Chen K, Khodakov A, Yang J, Bell AT, Iglesia E (1999) Isotopic tracer and kinetic studies of oxidative dehydrogenation pathways on vanadium oxide catalysts. J Catal 186:325–333. doi:10.1006/jcat.1999.2510
27. Gilardoni F, Bell AT, Chakraborty A, Boulet P (2000) Density functional theory calculations of the oxidative dehydrogenation of propane on the (010) surface of V_2O_5. J Phys Chem B 104:12250–12255. doi:10.1021/jp001746m
28. Nguyen NH, Tran TH, Nguyen MT (2009) Study of the adsorption step in the oxidative dehydrogenation of propane on V_2O_5 (001) using calculations of electronic density of states. Interdiscip Sci Comput Life Sci 1:308–314. doi:10.1007/s12539-009-0050-9d
29. Andersson A (1982) An oxidized surface state model of vanadium oxides and its application to catalysis. J Solid State Chem 42:263–275. doi:10.1016/0022-4596(82)90005-6
30. Kämper A, Hahndorf I, Baerns M (2000) A molecular mechanics study of the adsorption of ethane and propane on V_2O_5(001) surfaces with oxygen vacancies. Top Catal 11–12:77–84. doi:10.1023/A:1027239612464
31. Fu H, Liu ZP, Li ZH, Wang WN, Fan KN (2006) Periodic density functional theory study of propane oxidative dehydrogenation over V_2O_5(001) surface. J Am Chem Soc 128:11114–11123. doi:10.1021/ja0611745
32. Witko M, Hermann K (1993) Hydrogen adsorption and OH desorption at vanadium pentoxide surfaces: ab initio cluster model studies. J Mol Catal 81:279–292. doi:10.1016/0304-5102(93)80012-J
33. Ramirez R, Casal B, Utrera L, Ruiz-Hitzky E (1990) Oxygen reactivity in vanadium pentoxide: electronic structure and infrared spectroscopy studies. J Phys Chem B 94:8960–8965. doi:10.1021/j100389a021

34. Cheng MJ, Chenoweth K, Oxgaard J, Van Duin A, Goddard WA (2007) Single-site vanadyl activation, functionalization, and reoxidation reaction mechanism for propane oxidative dehydrogenation on the cubic V_4O_{10} cluster. J Phys Chem C 111:5115–5127. doi:10.1021/jp0663917
35. Nguyen NH, Tran TH, Nguyen MT, Le MC (2010) Density functional theory study of the oxidative dehydrogenation of propane on the (001) surface of V_2O_5. Int J Quantum Chem 110:2653–2670. doi:10.1002/qua.22389
36. Khaliullin RZ, Bell AT (2002) A density functional theory study of the oxidation of methanol to formaldehyde over vanadia supported on silica, titania, and zirconia. J Phys Chem B 106:7832–7838. doi:10.1021/jp014695h
37. Redfern PC, Zapol P, Sternberg M, Adiga SP, Zygmunt SA, Curtiss LA (2006) Quantum chemical study of mechanisms for oxidative dehydrogenation of propane on vanadium oxide. J Phys Chem B 110:8363–8371. doi:10.1021/jp056228w
38. Ha NN, Huyen ND, Cam LM (2011) Ab-initio study of effect of basic MgO to V_2O_5 catalyst on oxidative dehydrogenation of C_3H_8 and n-C_4H_{10}. Appl Catal A 407:106–111. doi:10.1016/j.apcata.2011.08.031
39. Perdew JP, Burke K, Ernzerhof M (1996) Generalized gradient approximation made simple. Phys Rev Lett 77:3865–3868. doi:10.1103/PhysRevLett.77.3865
40. Soler JM, Artacho E, Gale JD, García A, Junquera J, Ordejón P, Sánchez-Portal D (2002) The SIESTA method for ab initio order-N materials simulation. J Phys Condens Matter 14:2745–2779. doi:10.1088/0953-8984/14/11/302
41. Kanai Y, Wang X, Selloni A, Car R (2006) Testing the TPSS meta-generalized-gradient-approximation exchange-correlation functional in calculations of transition states and reaction barriers. J Chem Phys 125:234104–234112. doi:10.1063/1.2403861
42. Rappoport D, Crawford NRM, Furche F, Burke K (2009) Computational inorganic and bioinorganic chemistry, Wiley, Chichester. Wiley, John & Sons, Inc., Hoboken
43. Hamann DR, Schlüter M, Chiang C (1979) Norm-conserving pseudopotentials. Phys Rev Lett 43:1494–1497. doi:10.1103/PhysRevLett.43.1494
44. Berne BJ, Ciccotti G, Coker DF (1998) Classical and quantum dynamics in condensed phase systems. World Scientific, Singapore
45. Henkelman G, Uberuaga BP, Jónsson H (2000) A climbing image nudged elastic band method for finding saddle points and minimum energy paths. J Chem Phys 133:9901–9904. doi:10.1063/1.1329672
46. Zhai HJ, Dobler J, Sauer J, Wang LS (2007) Probing the electronic structure of early transition-metal oxide clusters: polyhedral cages of $(V_2O_5)n-$ (n=2–4) and $(M_2O_5)2-$ (M = Nb, Ta). J Am Chem Soc 129:13270–13276. doi:10.1021/ja0750874
47. Dong F, Heinbuch S, He SG, Xie Y, Rocca JJ, Bernstein ER (2006) Formation and distribution of neutral vanadium, niobium, and tantalum oxide clusters: single photon ionization at 26.5eV. J Chem Phys 125:164318–164325. doi:10.1063/1.2358980
48. Weckhuysen BM, Keller DE (2003) Chemistry, spectroscopy and the role of supported vanadium oxides in heterogeneous catalysis. Catal Today 78:25–46. doi:10.1016/S0920-5861(02)00323-1
49. Walter A, Herbert R, Hess C, Ressler T (2010) Structural characterization of vanadium oxide catalysts supported on nanostructured silica SBA-15 using X-ray absorption spectroscopy. Chem Cent J 4:3. doi:10.1186/1752-153X-4-3
50. Ganduglia-Pirovano MV, Sauer J (2004) Stability of reduced V_2O_5(001) surfaces. J Phys Rev B 70:045422. doi:10.1103/PhysRevB.70.045422
51. Rodella CB, Mastelaro VR (2003) Structural characterization of the V_2O_5/TiO_2 system obtained by the sol–gel method. J Phys Chem Solids 64:833–839. doi:10.1016/S0022-3697(02)00414-6
52. Avansi W, Ribeiro C, Edson R, Leite ER, Mastelaro VR (2009) Vanadium pentoxide nanostructures: an effective control of morphology and crystal structure in hydrothermal conditions. Cryst Growth Des 9:3626–3631. doi:10.1021/cg900373f